Journal of Sciences, Islamic Republic of Iran 23(4): 337-346 (2012) http://jsciences.ut.ac.ir
University of Tehran, ISSN 1016-1104

Determination of Coal Seams Depth of Erosion with Respect to the Remnants of a Key Bed in Kerman Coal Field, Iran

A. Elahi,[1,*] J. Shahabpour,[2] H. Ranjbar,[3] and S. Radfar[2]

[1]Department of Mining Engineering, Faculty of Zarand Industry and Mining, Shahid Bahonar University of Kerman, Islamic Republic of Iran
[2]Department of Geology, Faculty of Sciences, Shahid Bahonar University of Kerman, Islamic Republic of Iran
[3]Department of Mining Engineering, Faculty of Engineering, Shahid Bahonar University of Kerman, Islamic Republic of Iran

Received: 29 October 2011 / Revised: 9 June 2012 / Accepted: 9 October 2012

Abstract

As a tool for exploration of concealed coal seams by modern techniques, determination of the depth of erosion of coal seams with reference to the surface of angular unconformity underlying the remnants of a key bed is conducted for the first time in coal mines of Kerman region. The angular unconformity surface (the initial surface exposure of coal seams) separates the coal seams of Jurassic age from thick limestone beds of Cretaceous age (key bed) in the coal synclinorium of Kerman region. Frequent tectonic deformation in Cenozoic led to the exhumation of portions of Cretaceous limestone (key bed) together with the coal seams of Jurassic age. The initial surface exposure of coal seams which is referred to as the "initial surface" herein, determines the upper limit of the coal seams in Early Cretaceous and is used as a "reference surface". After importing and processing the available information, namely, satellite data, field survey data, geological maps, topographic and hypsometric data, Global Positioning System (GPS) data and geo-structural data of the reference surface and present surface exposure of coal seams into GIS software, the depth of erosion of coal seams between the "initial surface" (reference surface) before erosion and the "present surface" after erosion was calculated. It is concluded that the depth of erosion of coal seams in northern region is higher than the southern region. Therefore, the remnant of the coal seams (concealed coal seams) along the dip direction is higher in the south as compared to the northern sector. The results of this study are applicable to the future exploration in coal fields and similar deposits elsewhere.

Keywords: Angular unconformity; Depth of erosion; Coal seams; Kerman; Iran

Introduction

Kerman coal field is located in southeast of Iran, to the north of Kerman Province, between the longitudes 56° 30’ and 56° 75’ E and latitudes 30° 35’ and 31° N (Fig. 1). Geologically, the region is a part of the Central

* Corresponding author, Tel.: +98(341)3222035, Fax: +98(342)4202040, E-mail: alielahi29@yahoo.com

Iran geo-structural zone. The region is mountainous with an average elevation of 2500 meters above mean sea level. The climate is arid with hot summers and severe winters. The temperature ranges annually from -5°C to 45°C. The average precipitation is 165 mm/year [1].

With the development of Iran's industry, coal resources are increasingly in great demand. As a result, the remaining coal reserves diminish gradually with the present large scale exploitation. The main exploration targets of coal are concealed and unidentified. The erosional thickness of the beds related to angular unconformities can be investigated with different methods [2]. Determination of parameters which are shown in Figure 2 in an area of about 2000 km^2, makes coal prospecting by using the aerial photo-interpretation difficult. It is therefore important to explore remnant coal seams by taking advantage of modern remote sensing and GIS techniques [3, 4]. Satellite navigation systems have become much more accurate; thus expanding the role that Global Positioning System (GPS) that can play in providing survey controls from "initial surface" and "present surface" (Fig. 2) for detailed geological and isometric mapping, collection of geo-structural and digital exploration data. Besides the traditional methods of exploration and processing, new idea of exploration in this research and new software programs have allowed gathering of vast amount of necessery information and analysis for exploration studies of concealed coal seams in this area [5].

Geological Setting

There are many publications on the geology of Iranian coal fields, namely, Seyed Emammi [7], Razavi-Armagani and Moenoalsadat [8], Yazdi [9] and Shariat [10] in Alborz and Tabas coal fields, Shahabpour [1], Razavi-Armagani and Moenoalsadat [8], in Kerman coal field. The development and evolution of Mesozoic sedimentary basin in East-Central Iran were largely governed by the Late Triassic collision of the Central-East Iranian Microcontinent (CEIM) [11, 12, 13] which is a part of the Cimmerian microplate assemblage [14], with the Turan Plate (Eurasia), followed by subsequent post-Triassic rotational movements of CEIM of about 135° with respect to Eurasia [15, 16, 17]. In the course of the rotation, small oceanic basins started to open up around the CEIM in Early Cretaceous (Neocomian) times [18, 19] that were subsequently closed during the later part of the Late Cretaceous and Paleocene, in connection with the advance of the Arabian Plate and the closure of Neotethys [20]. The rotation also caused fragmentation of the CEIM into individual blocks (Lut, Tabas, and Yazd blocks) [21, 22]. The Kerman coal field is located in the western part of Lut block.

This basin (CEIM) with a connection to Palaeotethys was formed during the Triassic time. Significant palaeogeographical changes subsequently occurred as a result of the Early Cimmerian tectonic movements of the Late Middle-Late Triassic (Carnian-Norian) and played a major role in the geological history of Jurassic deposits in this area [23]. After the orogenic activities, faulting to the north and south of this area created a new

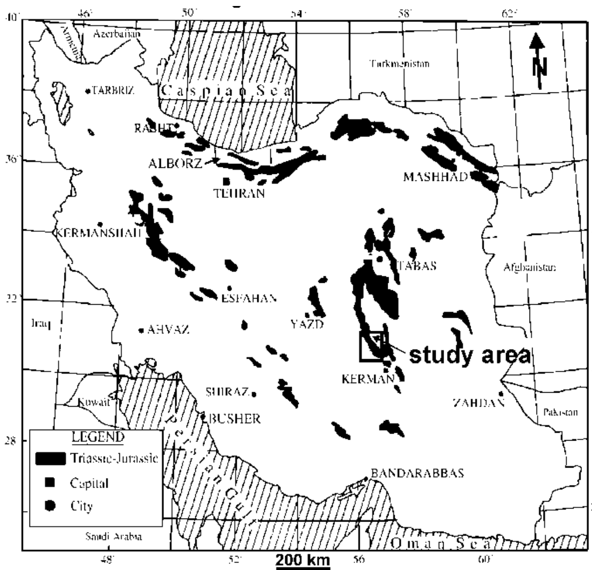

Figure 1. Distribution of Triassic-Jurassic outcrops (black) in Iran and location of study area. Redrawn after [6, 7].

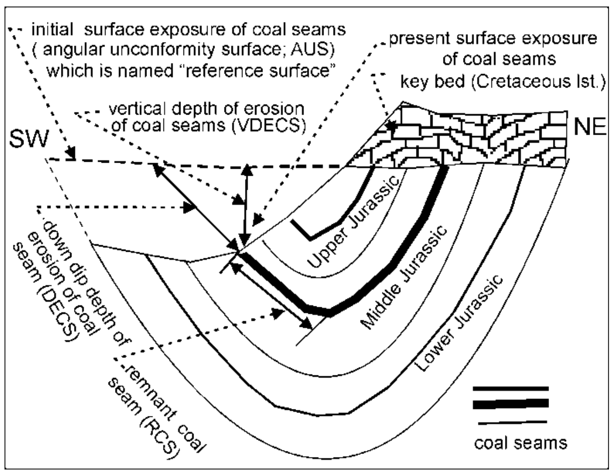

Figure 2. Schematic section showing geometric characteristics of coal seams in this study.

basin between the faults [24, 25]. The high amount of subsidence associated with these events caused deposition of thick sequence of terrigenous sediments that lasted until the Middle Cimmerian (Bajocian-Bathonian) [26] (Fig. 1). The detrital sediments in this basin vary in thickness from a few meters in south, up to more than 3000 m in the central part of Kerman coal field. These sediments are known as the Shemshak group (formerly the Shemshak Formation) which includes the Nayband, Badamu, Hojedk and Bidu Formations with coal bearing horizons of central part of Iran (Fig. 3) [26, 27, 28]. The Cretaceous sedimentary cycle starts with shallow to marginally marine and terrestrial facies across large area of the CEIM in the Late Cimmerian [26].

The Kerman coal field started to accumulate during the Late Barremian. It comprises of a thick sedimentary cover of lower Cretaceous platformal carbonate and shallow basinal (shales, marl, limestones) sediments (Fig. 3). The transgression which can be recognized across the Iranian plate, may be related to the marginal ocean basin development around the CEIM [18, 19]. An angular unconformity surface (AUS) (Figs. 2, 3, 4) separates the coal seams of Jurassic age from thick limestone beds of Cretaceous age in the coal synclinorium of Kerman region (Figs. 4a, 4b).

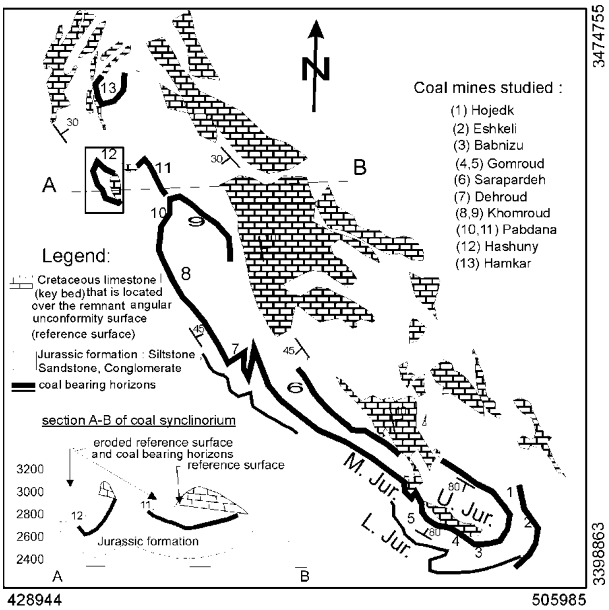

Figure 3. Geological and structural map of Kerman coal synclinorium (study area). Hashuny mine aera (No. 12) is magnified to show details. The rock units in the order of superposition are are: Lower Jurassic (L. Jur.), Middle Jurassic (M. Jur.), Upper Jurassic (U. Jur.) and Cretaceous Limestone (Cert. Lst.).

Frequent tectonic disturbances during Cenozoic led to folding, faulting, fracturing and exhumation of the portions of Cretaceous limestone and of the coal seams of Jurassic age [e.g., 29, 30]. The remnant Cretaceous limestone (the key bed) (Figs. 3, 4) has been studied by remote sensing (RS) techniques [e.g., 2, 3]. The remnant angular unconformity surface (reference surface) underlies the key bed. The region has experienced very different depositional histories during the Jurassic – Cretaceous, punctuated by major tectonic events [25, 26]. The geologic evolution of Kerman coal field is depicted in Figure 5.

Stratigraphy of Coal-Bearing Horizons

The Kerman coal field is located in the southwest of

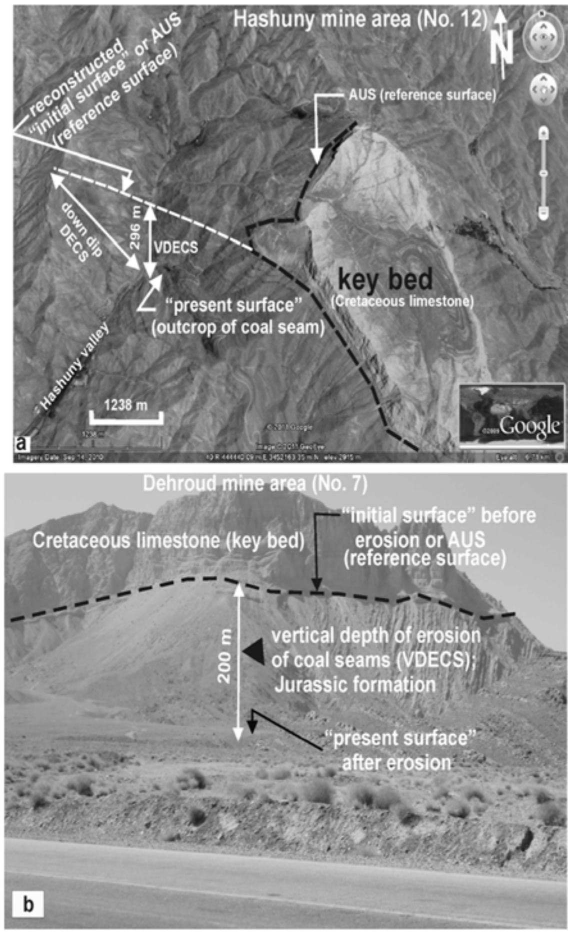

Figure 4. Position of "initial surface" or angular unconformity surface (reference surface) and "present surface" in two locations, from NW to SE; (a) A satelliate image of Hashuny mine (445953E, 3450744N and elevation of 2828 m); (b) Northwesterly view adjacent to Dehroud mine (472666E, 3435273N and elevation of 2560 m).

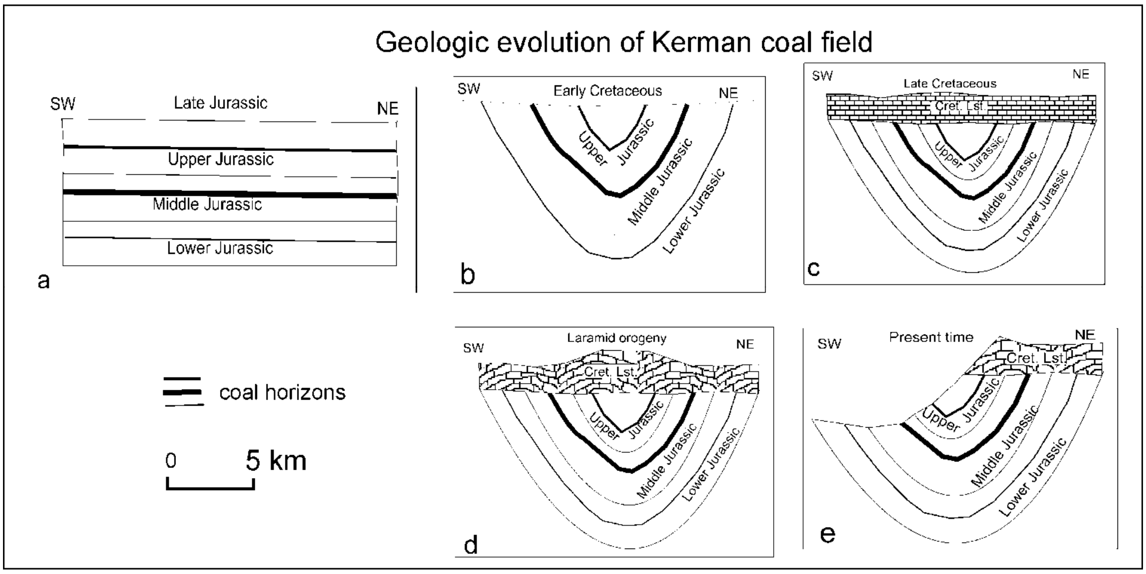

Figure 5. Schematic illustrations depicting the evolution of the study area. (a) Deposition of sedimentary horizons from Late Triassic to Upper Jurassic; (b) Folding in Late Jurassic Formation ; (c) Cretaceous Limestone unconformably overlying Upper Jurassic; (d) Laramide orogeny; (e) erosion of Cretaceous limestone beds, the surface of angular unconformity and coal bearing horizons . Abbreviations : *Cret. Lim*., Cretaceous Limestone.

Table 1. Stratigraphic sequence in Kerman coal mine region modified after (Salarisharif et al., 1983; Shahabpoure et al., 2005)

Epoch	**Stage**	**Series name**	***Age index***	**Thickness(m)**	**Coal zones**	**Exploitable subzones**	**Total thickness (m)**	**Operational thickness (m)**	**Coal Mines**
	Aptian								
	Albian	U. Cret.	K_2	50-300			------		
Cret.	Barmian								
	Titonian	L.Cret.	K_1	<50			------		
	Oxfordian								
			J_{3bd}						
		Bidu	J_{3as3}						
	Batonian	Asadabad	J_{3as2}	800-850			------		
			J_{3as1}		E	e_1,e_2,e_3,e_4,e_9	5.80		
	Bajocian	Dashtkhak	J_{2dsh}	180-1000			11.2	0.6	PD, HK
Jur.	Toarcian	Gomrud	J_{2gm2}	100-980	D	$d_1,d_2,d_3,d_4,d_5,d_6,d_9$	4	5.27	PD, HJ, HK, HS
			J_{2gm1}	135-200			----		
		Babnizu	J_{2bb}	60-250			-----		
		Neyzar	J_{1nz}	60-240					
			J_{1th3}	70-560	C_1		1.5	0.25	
			J_{1th2}	--------			------		
	Rhtian	Toqrajeh	J_{1th1}	150-600	C	c_5,c_7,c_8	5.21	2.64	BN, ES, PD
Tri.	Nornia	Darbidkhu	T_{3dr}	150-600	B_1	$b_{11},b_{12},b_{13},b_{14}$	0.85	0.1	------
			T_{3dh2}	160-600	B	b_4,b_9	5.03	0.33	BN, ES, HJ
	Carnian	Dehrud	T_{3dh1}	300-480	A		-----		DR, NZ, HJ, DB

Abbreviations: *BN*, Babnizu; *Cret*, Cretaceous; *DB*, Darbidkhun; *DR*, Dehrud; *Epo*, Epoch; *ES*, Eshkeli; Jur, Jurassic; *HJ*, Hojedk; *H*K, Hamkar; *NZ*, Nyzar; *P*D, Pabdana; *Tri*, Triassic

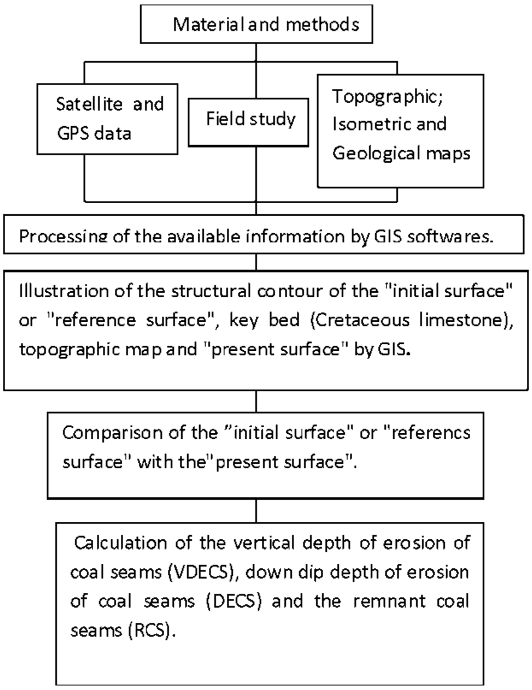

Figure 6. Flowchart for determination of the RCS in each limb of synclinorium with reference to the AUS (reference surface) and the DECS for Kerman coal field.

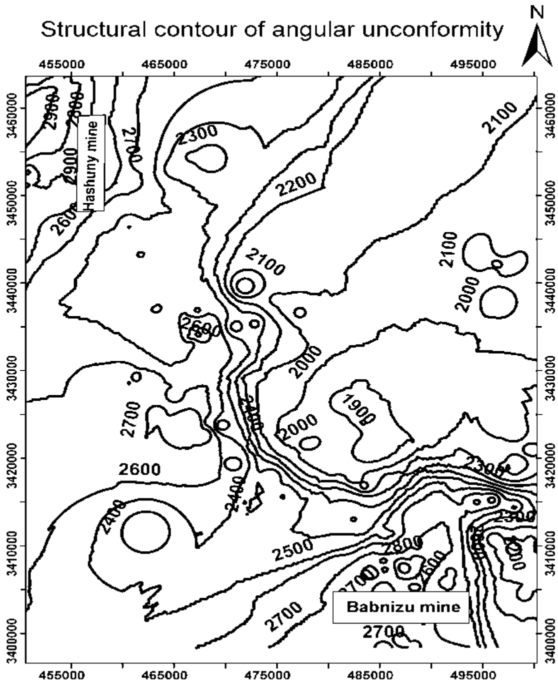

Figure 7. (a) Structural contour map of the surface of angular unconformity of Kerman coal synclinorium (study area) before erosion.

the Tabas Block and is bounded on the east by Darband dextral fault and on the west by Kuhbanan dextral fault [e.g., 1, 26, 30, 31]. The general trend of synclinal axis is NW-SE and its length is estimated at about 70 km. Deposition started from Late Triassic and lasted till Early Cretaceous, and includes the following lithostratigraphic units: Dehroud (Naiband), Nyzar-Babnizu (Shemshak), Badamu and Hojedk Formations [1, 8] (Table 1). These units in Kerman coal fields are together called the Jurassic Formation, and divided into three units namely, Lower Jurassic, Middle Jurassic and Upper Jurassic (Shemshak Group) (Fig. 3 and Table 1).

The coal bearing strata exist in six zones, namely, A, B, C, C´, D and E [1] (Table 1). The coal zones A and B are the oldest and belong to the Upper Triassic succession. The thickness varies from 1.25 m to 2.90 m. Coal zones C and C´ belong to the Lower Jurassic, with an average thicknesses of 5.21 m and 1.5 m, respectively. The coal zones D and E belong to the Middle Jurassic. Zone D with 20 coal seams contains the largest coal reserve which is subdivided into zones: d1, d2, d3, d4, d5, d6 and d9, out of which d1 and d2 are thicker than others. The overall thickness of d subzone is estimated to be 11.24 m. Thickness of zone E that is subdivided into zones: e1, e2, e3, e4 and e9 are estimated to be 5.80 m [1, 8, 32].

Materials and Methods

Data collection included the determination of geographic coordinates and geometric data for 400 points of the key bed (Cretaceous limestone), the "reference surface", initial surface and "present surface" by different methods, namely, GPS, satellite images (Enhanced Thematic plus (ETM+) data) and Digital Elevation Model (DEM), geological map (sheet Nos. 7351, 7352 in 1:100000 scale from Geological Survey of Iran and large scale geological maps of the mines in Table 1 from Kerman Coal Mines Company), hypsometric and topographic maps (in 1: 20000 scale from Kerman Coal Mines Company) and field observations [2, 3]. The geological maps and remote sensing images were geo-referenced using Universal Transverse Mercator (UTM) map projection and World Geodetic System (WGS84) as datum.

The maps were digitized by GIS software. Structural contours and polygons of part of eroded "reference surface", and remnant key bed were plotted. The elevation data were gridded using Kriging method and the reference surface was reconstructed. The raster images were also used for plotting of the crosssection profile of the present surface topography along the strike. These methods were used to determine downdip

Table 2. Geographic coordinates (X, Y) and elevation (Z) of the surface area of the "reference surface", coordinate system is in Universal Transverse Mercator (UTM)

points *1-30*			points 30-60			points 60-90			points 90-120		
Y N	*X* E	Z	*Y* N	*X* E	Z	*Y* N	*X* E	Z	*Y* N	*X* E	Z
3410573	481698	2500	3434157	467358	2747	3454656	447895	3090	3433491	466494	2552
3411931	462421	2325	3433759	466524	2644	3454659	447320	3025	3433045	466595	2437
3414043	481410	2310	3433148	465365	2434	3454612	446989	2983	3433091	465793	2421
3409298	485324	2674	3406982	491775	2575	3454909	446352	2952	3433165	465310	2439
3408326	485355	2821	3406243	491256	2573	3455132	447457	3157	3433591	464921	2416
3407514	487336	2976	3407799	489400	2773	3455257	446775	3051	3434070	464614	2435
3404278	487892	2805	3408121	488691	2879	3455310	446393	2965	3435443	463948	2445
3451834	444506	2914	3409598	487145	2677	3427414	474016	2088	3437135	463258	2533
3450988	444969	2910	3410030	486517	2653	3426082	474965	2063	3439058	462461	2477
3450460	445371	2912	3411327	486167	2452	3425105	475809	2009	3441497	462067	2450
3450665	445871	2900	3411056	486714	2597	3414471	483093	2300	3443252	461782	2513
3452174	445831	2717	3410571	487168	2637	3453672	456929	2932	3444747	461406	2433
3452149	444523	2842	3409878	488646	2667	3453572	459071	2723	3446384	460667	2502
3454709	447514	3104	3409212	489280	2779	3453896	461601	2539	3448611	460500	2502
3454656	448001	3125	3463346	441394	2675	3453110	464998	2350	3451112	459500	2668
3413311	482626	2312	3462560	441261	2696	3454377	466630	2288	3451488	458431	2773
3413403	482357	2366	3462139	441581	2752	3454196	468316	2225	3452935	456590	2926
3413540	482153	2388	3442113	461948	2454	3436894	467272	2384	3469739	446564	2530
3401872	499543	2278	3439254	462381	2465	3442038	496308	2271	3468308	444892	2625
3402226	499302	2232	3437592	462951	2469	3441460	496033	2034	3466939	443811	2783
3401541	499565	2348	3435606	463901	2462	3437973	474907	2082	3465813	442816	2795
3402046	498813	2247	3434945	464174	2413	3439572	471902	1916	3465157	442276	2609
3401789	498593	2277	3447101	460580	2465	3438567	496520	1943	3470693	439813	2647
3401321	498203	2391	3451325	459409	2705	3437121	475969	2071	3466702	440097	2726
3400679	499435	2379	3449488	459734	2559	3436655	477122	1965	3410573	481698	2500
3426530	474666	2078	3448799	460120	2519	3434924	474663	2204	3411931	481621	2325
3423690	477157	1954	3434702	467718	2628	3435348	472848	2431	3414043	481410	2310
3421599	478498	2053	3461000	442918	2796	3435017	471000	2254	3409298	485324	2674
3420458	479428	1930	3460473	443097	2702	3435091	467818	2524	3408326	485355	2821

depth of erosion of the coal seam (DECS), from Late Jurassic to Present, and to calculate the length of the remnant coal seams (RCS) in dip direction. The flowchart for data analysis is presented in Figure 6.

Results and Discusion

The surface area of "reference surface" is estimated at about 1500 km^2 in Early Cretaceous. Parts of the Cretaceous limestone is eroded and its remnant outcrops with steep slopes are scattered over an extensive area in this region (Figs. 4a, 4b). The present surface area of the remnant limestone bed is studied by remote sensing and is estimated by GIS method to be about 450 km^2 (Fig. 3). Therefore, area of the remnant "reference surface" which is located under the remnant Cretaceous limestone is estimated at about 450 km^2. Its outcrops occur with sharp contact with respect to the surface of angular unconformity all over the Kerman coal field synclinorium (Fig. 4). Contact of AUS is visible over a distance of about 280 km [2, 3].

Parameters which are used in this study are shown in Figure 3. Structural contours of the reference surface (AUS) can be reconstructed by using the interpolation of the measured data (Tables 2 and 3) which are derived from surveying, field studies, satellite images and DEM using GIS techniques. These data were geo-referenced and gridded by using GIS software.

Structural contours of "reference surface" were plotted (Fig. 7). The trace of coal seams before erosion (exposure of coal seam in Late Jurassic) is illustrated by using the geometric characteristics of the coal seams (Fig. 8a, parameters in section B-C in Figure 10 and data from Table 4). The topographic map of Hashuny mine area is provided by digital elevation model (Fig. 8b). A satellite image (Fig. 4a) from Hashuny mine shows the position of the "initial surface" (AUS) underneath the key bed with respect to the "present surface" (outcrop of coal seams).

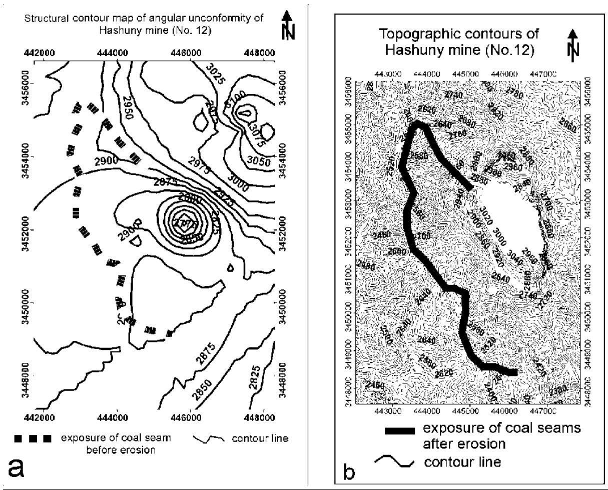

Figure 8. (a) Structural contour map of the surface of angular unconformity before erosion of Hashuny mine; b)Topographic contour map (present surface) after erosion of Hashuny mine. The thickness of coal seam is not to the scale.

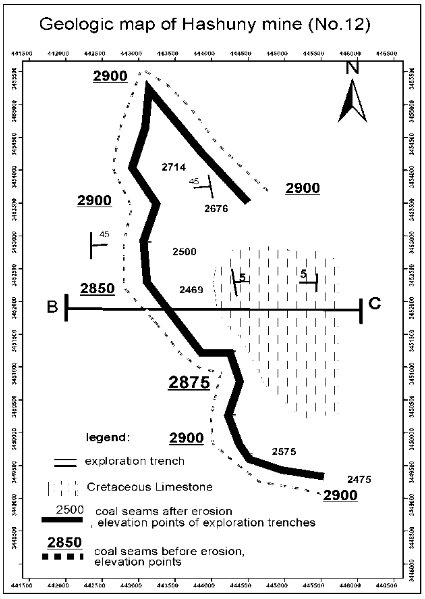

Figure 9. Geologic map of Hashuny mine (No. 12). The exposure of coal seams before and after erosion is shown.

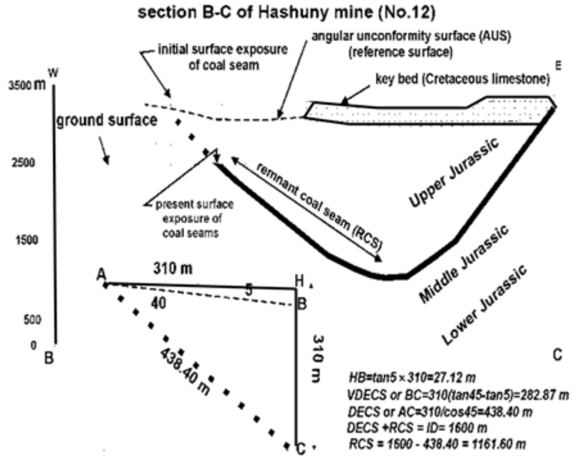

Figure 10. Section of Hashuny mine area from Figure 8. The geometric elements of the coal seams in AHC triangle, are namely; point A represents the "initial surface", point C represents the "present surface", AH represents the horizon, AB is the refrence surface (AUS); AC is perpendicular to the strike and parallels the dip direction of the coal seam (DECS); BC represents the VDECS.The dip of the angular unconformity surface is 5 degrees while the dip of the coal seams is 45 degrees.

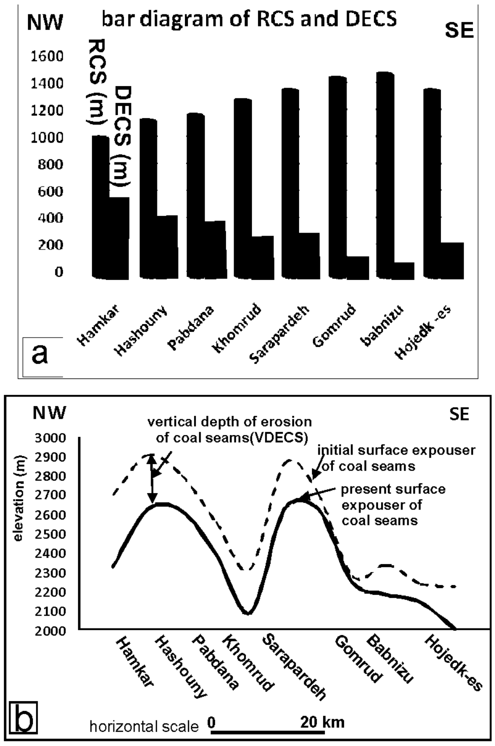

Figure 11. (a) Bar diagram of the DECS and the RCS values in coal mines**.** (b) Cross section of coal seams along axis of Kerman coal synclinorium from NW to SE showing the obtained "initial surface" before erosion and "present surface" after erosion.

The geographic coordinates of points of the "initial surface" before erosion and the "present surface" after erosion are presented in Table 3. These data were converted into raster format using data interpolation in GIS software (Fig. 8b). The calculated vertical depths of erosion of the coal seams (VDECS) are listed in Table 3 and summarized in Table 4. The map in Figure 9 is drawn by superimposing Figures 8a and 8b and depicts the surface exposure of the coal seams before and after erosion. Geometric characteristics (DECS, RCS) of coal seams in two dimensions are illustrated in section B-C of Hashuny mine area (Fig. 10). The average initial depth (ID) of coal seams in dip direction is reported to be bout 1600 m on both limbs of the synclinorium [34].The DECS and RCS were calculated by using equations in Figure 1.

Geometric components of coal seams in two dimensions are displayed in Figure 10. In the AHC triangle, the line AH is horizontal while the line AC is perpendicular to the strike and parallel to the dip direction of the coal seam (DECS). The line BC indicates the vertical depth of erosion of the coal seams (VDECS), whereas the line AB represents the surface of angular unconformity (reference surface), and the dip angle of angular unconformity surface (reference surface) is 5 degrees while the dip angle of coal seams is 45 degrees.

Calculations of the DECS and the RCS for other mines were carried out as in Hashuny mine and the overall results are summarized in Table 4.

In the mines located in the northwest (Hamkar, Hashuny and Pabdana in Table 4) , the average surface elevations of the "initial surface"(the reference surface) and the "present surface" are 2800 and 2523 m, respectively. These are the average values of "initial surface" and "present surface" for the said mines in Table 4. The dip of coal seams is less than 45 degrees. Based on the average downdip DECS values of the first three mines in Table 4 (Fig. 11), the downdip of DECS is about 469 m for these mines.

In the southeastern mines (Gomrud, Babnizu, Hojedk-Eshkeli mines in table 4) the average surface elevations of the "initial surface" (reference surface) and the "present surface" are 2454 and 2308 m, respectively. The dip of coal seams is more than 45 degrees. Downdip, the DECS is about 160 m (Fig. 11, Table 4). Depth of erosion of coal seams decreases from NW to SE (Fig. 11) and as a result the coal seams are less eroded as compared to those on the northwest sector (Fig. 11b).

Based on the data presented in Table 4, the bar diagram in Figure 11 is plotted. The DECS decreases while the RCS (concealed coal seams in every limbs of synclinorium) increases from NW to SE (Fig. 11a).

Cross section of coal seams along the axis of Kerman coal synclinorium from NW to SE (Fig. 11b) depicts both "initial surface" before erosion and "present surface" after erosion. The decrease in elevation of "reference surface" (initial surface) from the NW to SE sectors is exemplified by Hashuny (2903 m), Sarapardeh (2313 m) and Hojedk mines (2228 m), respectively (Table 4), as the DECS decreases from NW to SE.

Based on the DECS and RCS data presented in Table 4, Kerman coal field area can be divided into two distinct sectors namely, northwest sector (comprising of Hamkar, Hashuny Pabdana mines) and southeast sector (comprising of Gomrud, Babnizu and Hojedk mines). Due to a higher depth of erosion in the NW sector of the synclinorium compared to SE sector, the latter contains larger number of concealed coal seams at higher depth (Fig. 6b). However, the coal seams are located at an

Table 3. Geographic coordinates (X ,Y) and elevation (Z) of points of "initial surface" (IS) and "present surface" (PS) (outcrop of coal seams) in Hashuny mine area (No.12). Vertical depth of erosion of coal seam (VDECS) is calculated from the "initial surface" minus the "present surface"

X	Y	IS (m)	PS (m)	VDECS= IS-PS (m)
444552	3453556	2900	2677	223
444181	3453847	2905	2644	261
443791	3454370	2930	2676	254
443383	3454927	2910	2693	217
443118	3455239	2910	2743	167
443093	3454620	2915	2725	190
442947	3454051	2915	2714	201
443247	3453447	2895	2544	351
443128	3452905	2890	2500	390
443109	3452344	2890	2469	421
443872	3451246	2890	2692	198
443134	3452210	2880	2469	411
443609	3451616	2890	2594	296
444286	3451243	2890	2727	163
444384	3450792	2915	2662	253
442263	3450570	2910	2629	281
444281	3450268	2910	2607	303
444350	3449824	2905	2566	339
444519	3449672	2905	2575	330
444939	3449440	2905	2517	388
Average:		**2903**	**2621**	**282**

Table 4. The downdip depth of erosion of coal seams (DECS) and the downdip remnant coal seams (RCS) in each limb of synclinorium in various coal mines

Mines	Coordinates of Initial and end of Mine area	Average Elevation IS, PS (m)	VDECS (m)	Dip and dip Dir. (degree)	Down dip DECS (m)	Down dip RCS (m)
Hamkar	446910/3469084 445152/3467285	2696 2332	364	45/135 45/305	568	1032
Hashuny	442915/3455395 445492/3449358	2903 2621	282	45/90 45/270	439	1161
Pabdana	449134/3455274 449380/3442377	2800 2617	180	30/45	400	1200
Khomrud	445250/3450750 460500/3439000	2556 2393	163	38/290	291	1309
Sarapardeh	470748/3425608 472824/3423143	2313 2093	220	50/290	314	1286
Gomrud	484307/3409537 488012/3405095	2764 2626	138	80/45	143	1457
Babnizu (M., N.,E.)	486820/3403750 497500/3404000	2390 2300	90	80/5	95	1505
Hojedk-Eshkeli	498323/3412913 500309/3403185	2228 2003	215	70/320	241	1359

Abbreviations: *D E*, eastern; *IS, "* Initial surface"; *La*, Latitude; *Lo*, Longitude; *M*, main; *N*, Northern; *PS*, "Present surface"

intermediate depth in the central sector (Fig. 6a). This is deduced from the southeastward inclination of the synclinorium axis as well as the steeper topography in the northwest sector as compared to the southeast sector.

Based on Figure 11b the erosional surface reflects the "initial surface" (the angular unconformity surface). This suggests that the local geological factors might not have influenced the erosional processes. In fact the erosional processes can be attributed to a regional factor that might be orogenic in nature. The shallower dip and the larger apparent thickness of soft beds in the northwest sector as compared to that of the southeast sector led to a higher degree of weathering in the northwest sector. Furthermore, the higher altitudes of the northwest sector led to a higher erosion of this sector as compared to the southeast sector.

Acknowledgments

The authors are grateful to Kerman Coal Mines Company for providing the geological reports and maps. We thank the referees of the journal of sciences for their valuable comments. Dr. Anoushirvan Lotfali Kani is thanked for editing the text. This work was financially supported by Shahid Bahonar University of Kerman.

References

1. Shahabpour J., Doorandish M., Abbasnejad A. Mine-drainge water from coal mines of Kerman region, Iran. Environmental Geology **47**, 915-925 (2005).
2. Lin, C., Yang, H., Liu, J., Rui, Z., Cai, Z., Zhu, Y. Distribution and erosion of the Paleozoic tectonic unconformities in the Tarim Basin, Northwest China: Significance for the evolution of Paleo-uplifts and tectonic geography during deformation. Journal of Asian Earth Sciences **46**, 1-19 (2012).
3. Tan K L., Wan Y Q., Sun S X., Bao G B., Kuang J S. Prospecting for coal in China with remote sensing, Journal of China University of Mining & Technology **18**, 537-545 (2008).
4. Anupma, P., Zohan, V. Design and implementation of a dedicated prototype GIS for coal fire investigations in North China. International Journal of Coal Geology **59**, 107-119 (2004).
5. Adeli Sarcheshme A., Karimi M., Bahroudi A., Elyasi G. Determination of drilling point of the Chahfirozeh prospect using fuzzy logic in GIS. Journal of Science, University of Tehran (in Persian) Vol. **35**, 85-97 (2009).
6. Goodarzi F., Sanei H., Stasiuk L.D., Bagheri-Sadeghi H., Reyes J. A preliminary study of mineralogy and geochemistry of four coal samples from northern Iran. International Journal of Coal Geology **65**, 35-50 (2006).
7. Seyed-Emami, K. Stratigraphy, Palaeobiogeography and palaeogeography of the "Middle Cretaceous strata" (Barremian-Albian) in Central Iran. Quaternary Journal of the Geological Survey of Iran **6 (21/22),** 50-69 (1997).
8. Razavi-Armagani, M.B., Moenoalsadat, S.H. Treatise on the Geology-Geological Survey of Iran, P. 286 (in Persian) (1994).
9. Yazdi, M.,Shiravani, A.E. Geochemical properties of coals in the Lushan coal field of Iran. International Journal of Coal Geology **60**, 73-79 (2004).
10. Yazdi, M., Esmaeilnia, S.A. Dual-energy gamma-ray technique for quantitative measurement of coal ash in the

Shahrud mine, Iran. International Journal of Coal Geology **55**, 151-156 (2003).
11. Takin, M. Iranian geology and continental drift in the Middle East. Nature, **235**, 147-150 (1972).
12. Poole, I., Mirzaie Ataabadi M. Conifer woods of the Middle Jurassic Hojedk Formation (Kerman Basin) Central Iran. IAWA Journal, vol. **26(4),** 489-505 (2005).
13. Schweitzer H. J., Kirchner M., Van Konijnenburg-Van C. The ratio Jurassic flora of Iran and Afghanistan, Bryophyta, Lycophyta, Sphenophyta-Eusporangiatae. Palaeontographica **B 243**, 103-192 (1997).
14. Sengor, A.M.C. A new model for the late Palaeozoic-Mesozoic tectonic evolution of Iran and implication for oman. In: Robertson, A.H.F., Searle, M.P., Ries, A.C. (Eds), the geology and tectonics of the oman region. Geological Society of London, Special publication **49**, 797-831 (1990).
15. Sofel, H., Förster, H., Polar wander path of the Central East Iran microplate including new results. Neues Jahrbüch für Geologie und Paläontologie, Abaandlungen, **168**, 165-172 (1984).
16. Davoudzadeh, M., Sofel, H., Schmidt, K., On the rotation of the Central-East Iran microplate. Neues Jahrbüch für Geologie und Paläontologie, Monatshefte **3**, 180-192 (1981).
17. Alavi, M., Vaziri, H., Seyed-Emami, K., Lasemi, Y. The Triassic and associated rocks of the NakAghdarband areas in central and northeastern Iran as remnants of the southern Turan active continental margin. Geological Society of America Bulletin **109**, 1563-1575 (1997).
18. Seyed-Emammi K., Bozorgnia F., Eftekakhar-Nezad J. Der erste sichere Nachweis von valanginien im nordlichen Zentraliran, Sabzewar-Gbiet. Neues Jahrbüch für Geologie und Paläontologie, Monatshfte **1,** 52-67 (1972).
19. Lindenbe H.G., Jacobshagen V. Post-Paleozoic geology of the Taknar Zone and adjacent areas (NE Iran, Khorasan). Geological Survey of Iran, Rport **51**, 145-163 (1983).
20. Tirrul, R., Bell, I.R., Griffis, R.J., Camp, V.E. The Sistan suturezone of eastern Iran. Geological Society of America, Bulletin **94**, 134–150 (1983).
21. Evgenij., Baraboshkin., Alexander., Alekseeve S., Ludmila., Kopaevich F. Cretaceous Palaeogeography of the North-Eastern Peri-Tethys. palaeogeography, palaeoclimatology, Palaeoecology **196**, 177-208 (2003).
22. Seyed-Emami K., Fursich F.T., Wilmsen M. Documentation and significance of tectonic events in the northern Tabas Block (east-central Iran) during the Middle and Late Jurassic. Rivisa Italiana di Paleontologia, Stratigrafia **110**, 163-171 (2004).
23. Li, D.S., Liang, D.G., Jia, C.Z., Wang, G., Wu, Q.Z., He, D.F. Hydrocarbon accumulation in the Tarim Basin, China. In; Lin, C., Yang, H., Liu, J., Rui, Z., Cai, Z., Zhu, Y. Distribution and erosion of the Paleozoic tectonic unconformities in the Tarim Basin, Northwest China: Significance for the evolution of Paleo-uplifts and tectonic geography during deformation. Journal of Asian Earth Sciences **46**, 1-19 (2012).
24. Shahabpour J. Liesegang blocks from sandstone beds of the Hojedk Formation, Kerman, Iran. Geomorphology **22**, 93-106 (1998).
25. Shahabpour J. Liesegang Ring, in Goudie A.S. (ed). Encyclopedia of Geomorphology Vol. **2**, 620-621 (2004).
26. Berberian M., King G. Towards a paleogeography and tectonic evolution of Iran. Canadian Journal of Earth Sciences **18**, 210-265 (1981).
27. Wilmsen M., Wiese F., Seyed–Emami, K., T.Fursich, F. First record and significance of Touronian ammonites from the Shotori Mountains, east-central Iran. Cretaceous Research **26**, 181 (2003).
28. Naimi Ghassabiyan N., Saidi A., Aghanabati A., Qorashi M., Ghasemi M.R. Geohistory Analysis of the Tabas Block (Abdoughi-Parvadeh Basins) as seen from the Late Triassic through Early Cretaceous Subsidence Curves. Journal of Science, Islamic Republic of Iran **21(1)**, 49-63 (2010).
29. Coakley, B., Watts, J., Coakley, A., Watts, B. Tectonic controls on the development of nconformities; the North Slope, Alaska, Tectonics, **10 (1)**, 10-130 (1991).
30. Paola, C., Domenico, C. Miocenen unconformity in the Central Apennines:geodynamic significance and sedimentary basin evolution. Tectonophysics, **252**, 375-389 (1995).
31. Elahi A., Shaker Ardekani A., Iranmanesh M. Study of reconstruction zones after Zarand earthquake 2005 from local position point of view (in Persian). The First Conference on Seismology and Earthquake Geodynamics, Kerman, Iran **(SEG. 1**), 1-5 (2010).
32. Elahi A., Shaker Ardekani A., Taraz H., Iranmanesh M., Shafiei A. Investigation of corelative effieciency of local position and lightweight construction based on 1977 and 2005 Zarand Earthquakes (in Persian). Proceedings of International Conference on Lightweight Construction and Earthquake, Kerman, Iran Vol. **1**, 556-563 (2010).
33. Salarisharif, H. Summary report of coal mines of Kerman region (in Persian), In Proceedings of the First Iranian Mining Symposium, Kerman. 43 pp. (1983).
34. Karamashyf K., A review of Kerman coal field geology. Kerman coal mining company **1**, 1-70 (1973).